PHYSICAL REVIEW B, VOLUME 63, 060103(R)

Critical behavior in spallation failure of metals

Alejandro Strachan, Tahir Çağın, and William A. Goddard III*
Materials and Process Simulation Center, Beckman Institute (139-74), California Institute of Technology, Pasadena, California 91125
(Received 30 October 2000; published 23 January 2001)

Using molecular dynamics with an accurate many-body potential, we studied the rapid expansion of Ta metal following the high compression (50 to 100 GPa) induced by high velocity (2 to 4 km/s) impact. We find that catastrophic failure in this system coincides with a critical behavior characterized by a void distribution of the form $N(v) \propto V^{-\tau}$, with $\tau \sim 2.2$. This corresponds to a threshold in which percolation of the voids results in tensile failure. We define an order parameter (ϕ, the ratio of the volume of the largest void to the total void volume) which changes rapidly from ~ 0 to ~ 1 when the metal fails and scales with as $\phi \propto (\rho - \rho_c)^{\beta}$ with exponent $\beta \sim 0.4$, where ρ is the total void fraction. We found similar behavior for FCC Ni suggesting that this critical behavior is a universal characteristic for failure of solids in rapid expansion.

DOI: 10.1103/PhysRevB.63.060103 PACS number(s): 62.50.+p, 62.20.Fe, 62.20.Mk, 64.60.Ht

Despite much progress in characterizing and analyzing the mechanical processes controlling the strength of materials, there are still many uncertainties regarding the dynamic failure of metals, particularly for the atomistic phenomena underlying macroscopic failure. To study such process at the atomistic level, we developed a first principles-based force field (FF) for Ta. We then applied this FF to examine dynamic failure using a high velocity plate colliding with a static target. Upon impact compressive waves travel both into the target and projectile. When these waves reach the free surfaces they reflect, becoming tensile, and propagate back into the material. When the two tensile waves meet, the material is subjected to a high tension, and for sufficiently high impact velocity the material will fail dynamically. This process, known as spallation, leads to failure of the material through formation, growth, and coalescence of microvoids or cracks.

Spallation has been studied extensively both experimentally and theoretically. The most widely used experimental methods are plate impact[1] and, more recently, high power pulsed laser shock generators.[2–6] Strain rates up to 10^8 sec^{-1} can be achieved with laser shocks, higher than those in plate impact experiments.

A complete description of spallation involves understanding and linking processes taking place at very different time and space scales, ranging from atomic size (vacancy coalescence and initial void formation) to microns (plastic deformation and linkage of micron-sized voids). Consequently theoretical studies of spallation have used methods ranging from microscopic molecular-dynamics (MD) simulations,[7] to mesoscale micromechanical models and continuum descriptions.[1,8,9]

We report here a MD study of the initial stages of spallation (length scales of nm and time scales of ps) that provides a detailed atomistic description for the time evolution of the process. We focus on characterizing the dynamical evolution of the void distribution.

To simulate high velocity impact, we assign a specific relative velocity to previously thermalized (perfect crystals at 300 K) projectile and target materials. We impose periodic boundary conditions to our system in the two directions perpendicular to the impact velocity and free boundary in the load direction, in this way we simulate two ''infinite'' plates. We then describe the collisional process using adiabatic MD simulations. We studied spallation in bcc Ta and fcc Ni. For Ta the projectile contains $N_p = 8192$ atoms per periodic simulation cell [$16 \times 16 \times 16$ unit cells, $\sim (53.25^3$ Å$)^3$] and the target $N_t = 16\,384$ ($32 \times 16 \times 16$ unit cells). For Ni we considered $N_p = 8788$ [$13 \times 13 \times 13$ unit cells, (~ 46 Å$)^3$] and $N_t = 17\,576$ ($26 \times 13 \times 13$ unit cells). We considered a variety of impact velocities (v_{imp}) (relative velocity between target and projectile) from 2 to 4 km/s (the sound velocity in Ta is ~ 3.4 km/s). For Ta, we use an embedded atom model FF fitted to accurate quantum mechanical calculations (QM).[10] For Ni we used an empirical many-body QSC (quantum Sutton-Chen) FF (Ref. 11) used previously for simulations of plasticity in Ni, and also a simple two-body Morse FF.[12]

Figure 1 shows snapshots of the process at different times for Ta with impact velocity of 2 km/s. The dots represent atomic positions projected on a [100] plane. Figure 1(a) shows the initial state of the system. Figure 1(b) shows the system at 2 ps when the system is compressed; Fig. 1(c) shows time 5.25 ps, at this time the system is expanding. Figures 1(d) and 1(e) show times $t = 6.5$ ps and $t = 7.25$ ps, where we can see the spall plane and void growth.

The aim of this work is to understand the dynamical evolution of voids in spallation and its relation to such macroscopic quantities as stress and failure. We consider a void as a connected empty region in the material which is separated from other voids by atoms. We define ''connected'' and ''separated by atoms'' as follows: (i) we map the space containing the atoms onto a cubic grid, with the grid spacing ($R_g = 0.52$ Å for Ta) about five times smaller than the distance between nearest-neighbor atoms ($R_{nn} \sim 2.88$ Å for Ta). (ii) We ''fill'' the grid points which contain an atom, by marking all the grid points closer to an atom than some atomic radius R_{at} (1.56 Å $\sim 0.54 R_{nn}$ for Ta). (iii) we define voids as connected clusters of empty sites: two empty sites belong to the same cluster if it is possible to go from one to the other through empty sites with (simple cubic) nearest-neighbors jumps. (iv) After filling the sites corresponding to the positions of all atoms, we also fill all the empty sites which contain more than one filled nearest-neighbor site; this

 ©2001 The American Physical Society

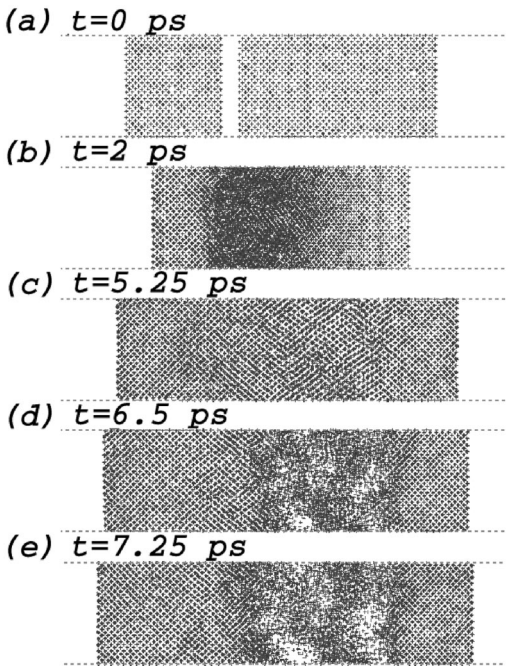

FIG. 1. Ta with $v_{imp}=2$. Snapshots of the spall process at different times. The dots represent atomic positions projected in a [100] plane. (a) Initial configuration; (b) $t=2$ ps when the system is compressed after the collision; (c) $t=5.25$ ps expansion stage; (d) and (e) $t=6.5$, and $t=7.5$ ps, respectively, the spall plane and void growth can be seen.

is done to ensure that no voids are found when the atoms are in their perfect crystal positions.

We tested this procedure by analyzing equilibrium (300 K, 432 atoms) MD runs for three different cases: i) perfect crystal, ii) crystal with one vacancy, and iii) crystal with a divacancy (two vacancies in nearest-neighbor sites). For Ta with lattice parameter $a=3.328$ Å (atomic volume $V \sim 18.43$ Å^3) we found: (i) perfect case: no volumes larger than ~ 0.6 Å^3; (ii) monovacancy case: we found one void of ~ 15 Å^3; and (iii) divacancy case: one void of ~ 27 Å^3. Thus we conclude that the void definition matches physical expectations.

Figures 2(a) and 2(b) shows the void volume distribution $N(V)$ (the number of voids as a function of volume) for Ta with $v_{imp}=2$ km/s at different times during the initial stage of the process. The void distributions shown were averaged over bins with bin limits given by $V_g 2^i$ with $V_g=R_g^3$ and $i=0,1,2\ldots$. In the initial stage of void nucleation, the distribution decays rapidly with volume (negative curvature), leading only to small voids [see $t=4$ ps in Fig. 2(a)]. This distribution broadens as voids coalesce and deform plastically, see times 4.25 and 4.5 ps in Fig. 2(a). At time $t_c=5.25$ ps [filled squares in Fig. 2(a)] the void distribution has a power law form for a wide volume range:

$$N(V)=N_0 V^{-\tau}, \tag{1}$$

with an exponent $\tau=2.2\pm0.05$ [shown by the thick line in Fig. 2(a)]. The deviations from the power law for small and large volumes will be explained below. In Fig. 2(b) we show

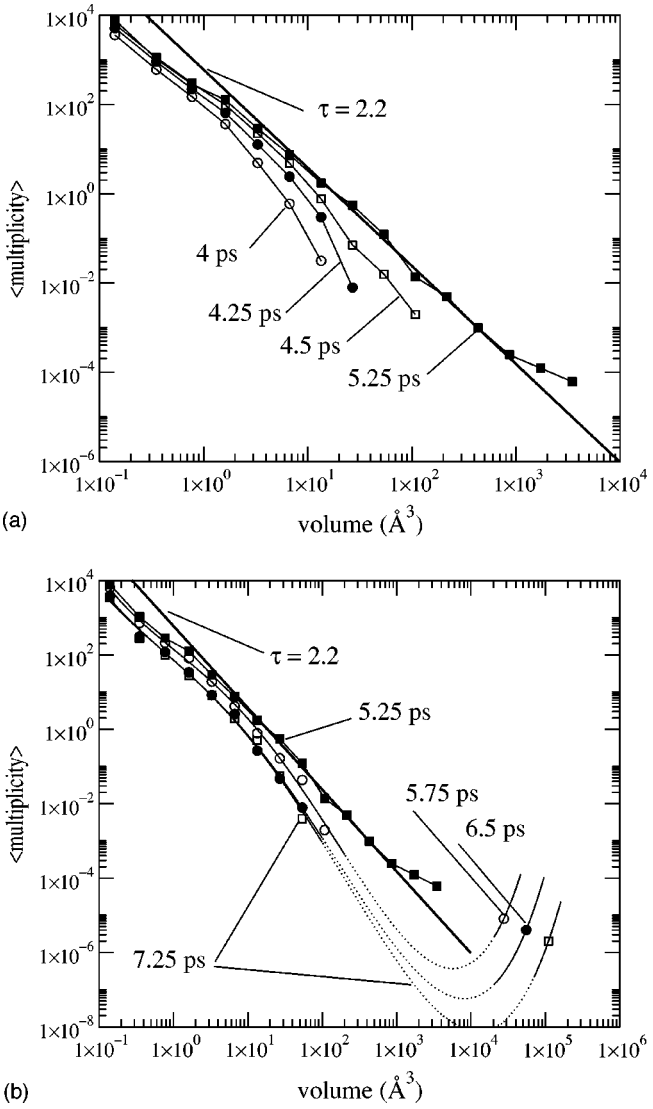

FIG. 2. Ta with $v_{imp}=2$. (a) Void volume distribution for the initial stages of the process. $t=4$ ps (empty circles), $t=4.25$ ps (filled circles), $t=4.5$ ps (empty squares) and $t_c=5.25$ ps (filled squares). We see that at $t=t_c$ the volume distribution follows a power law (the thick line shows a power law with exponent $\tau=2.2$). (b) Void volume distribution for the late stages of the process. $t_c=5.25$ ps (filled squares), $t=5.75$ ps (empty circles), $t=6.5$ ps (filled circles), and $t=7.5$ ps (empty squares). We see the growth of the largest void at the expense of the intermediate and low volume ones.

the void volume distribution for the late stage of the process, times 5.25, 5.75, 6.5, and 7.25 ps. We can see for times longer than 5.25 ps, a large void appears, leading to positive curvature in the void distribution for large voids, but negative curvature for small and intermediate volume voids (similar to the initial stages). It is clear from Figs. 2(a) and 2(b) that the void distribution has a special character at time $t_c \sim 5.25$ ps.

Figure 3(a) shows the time evolution of the volume of the largest void, V_{max}, and Fig. 3(b) shows the stress in the load direction as a function of time for Ta with $v_{imp}=2$ km/s. During the initial stages, for which the target and projectile

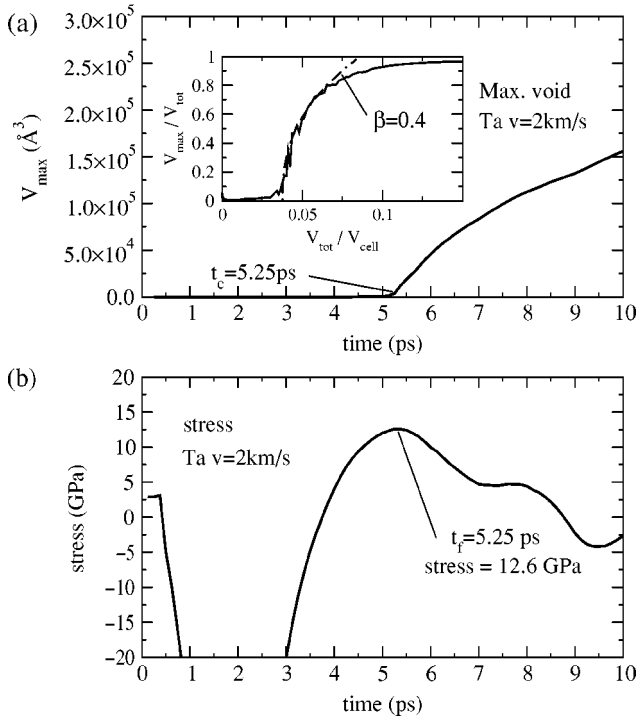

FIG. 3. Ta with $v_{imp}=2$. (a) Time evolution of the volume of the largest void and; inset: strength of the largest cluster as a function of total void concentration. (b) Stress in the load direction as a function of time. The maximum stress in compression (not shown) is ~ -46 GPa. The failure time $t_f \sim 5.3$ ps is very similar to the time $t_c=5.25$ ps at which the volume of the largest void starts growing.

are under compression, the stress attains large negative values (~ -50 GPa). During this stage the volume of the voids is almost zero. As the system expands the compressive stress relaxes and becomes tensile (positive stress or negative pressure), until the metal starts to fail (at $t_f \sim 5.25$ ps) and the stress drops from its maximum of ~ 12.6 GPa. Figure 3(a) shows that the behavior of the maximum void volume exhibits two different regimes; it remains very small during the initial stages of the process until at a critical time t_c its slope increases abruptly as the largest void starts growing very fast. Figures 3(a) and 3(b) show the clear relation between the presence of a large void and the failure of the material.

We define (i) *the strength of the largest void* as $\phi = V_{max}/V_{tot}$, where V_{max} is the volume of the largest void and V_{tot} is the total volume contained in voids; and (ii) the *total void concentration* as $\rho = V_{tot}/V$, where V is the total volume of the system.

The inset of Fig. 3(a) shows ϕ as a function of ρ. It is clear that there is a critical void concentration ρ_c at which the strength of the largest void starts to grow steeply. For $\rho \rightarrow \rho_c^+$ (from above), ϕ follows:

$$\phi \propto (\rho - \rho_c)^{\beta}, \tag{2}$$

with $\beta = 0.4 \pm 0.04$ (the dash-dot line in the inset of Fig. 3(a) shows $\beta = 0.4$).

For Ta with $v_{imp}=3$ km/s, the void volume distribution shows the same behavior; it follows a power law at $t_c = 4.125$ ps with the same exponent $\tau \sim 2.2 \pm 0.05$. This time correspond to the point of largest void growth, and is very close to the failure point $t_f \sim 4.2$ with a maximum stress of 9.45 GPa. The strength of the largest void, ϕ also follows Eq. (2) with $\beta \sim 0.4 \pm 0.04$.

We find similar void distribution behavior for Ni described with either the QSC FF or the Morse FF. For Morse Ni with $v_{imp}=2$ km/s we find power law behavior of the void volume distribution for $t \sim 3.1$ ps, the associated critical exponent is $\tau = -2.2 \pm 0.8$. In this case the exponent associated with ϕ [Eq. (2)] is $\beta = 0.4 \pm 0.08$. We found the same behavior for Morse Ni with $v_{imp}=3$ km/s and $v_{imp}=4$ km/s and for QSC FF for Ni at different impact velocities. In all cases we found $\tau \sim 2.2$ and $\beta \sim 0.4$. Thus, the general behavior for Ni (even described by a simple two-body force field) is the same as for Ta.

The power law behavior of the void distribution at the critical point for failure is very similar to the distribution of clusters in the percolation model at the critical probability[13] and the distribution of liquid drops in a liquid-vapor phase transition at the critical point.[14] The nonequilibrium process of fragmentation also shows power-law mass distribution and signals of critical behavior, see Refs. 15–17 and references therein. The mass distributions deviate from the power law for small and large masses, due to failure of scaling for small masses and finite-size effects for large masses.

The exponent τ is one of the critical exponents which determine the behavior of the system near the second-order phase transition. For three dimensional percolation $\tau = 2.2$,[13] and for the three-dimensional liquid-gas phase transition the exponent is $\tau \sim 2.33$.[14]

An essential characteristic to describe second-order phase transitions is an ''order parameter'' which is zero on one side of the phase transition (usually the high-temperature phase), and grows very rapidly (but continuously) to a finite value on the other side. The order parameter measures the difference between the system at opposite sides of the phase transition. In the case of the ferromagnetic-paramagnetic phase transition the order parameter is the spontaneous magnetization, [zero for $T > T_c$ (in the absence of external magnetic field), and nonzero at lower T, denoting spontaneous magnetization]. For liquid-gas phase transition the order parameter is the density difference between the coexisting liquid and gas. In these cases the order parameter follows Eq. (2) with exponent $\beta \sim 1/3$.

Our simulations show that the order parameter for spallation should be defined as the strength of the largest void, ϕ. The order parameter in percolation is defined in a similar way and its associated critical exponent is also $\beta = 0.4$.[13] From Fig. 3 we see that a nonzero order parameter indicates the failure of the material. A phenomenological micromechanical model developed to describe the void-link up effects in ductile fracture[8] and analysis of recent experiments also suggest similar percolationlike behavior at high strain rates.[1]

Summarizing, using MD simulations of high velocity impact, we find that spallation failure of the metals at high

strain rates corresponds to a critical point in which the distribution of voids follows a power law behavior with exponent $\tau \sim 2.2$. Our results suggest that the order parameter is defined by the ratio of the volume of the largest void to the total volume contained in voids. This order parameter follows the expected power law behavior near the critical concentration of voids with exponent $\beta \sim 0.4$ similar to the values found in percolation and the liquid-gas phase transition. We obtained similar results for Ta (represented by a many body force field) and Ni using both a simple two-body and a many body potential. The implication is that spallation failure of metals exhibits critical behavior. This is relevant for spall failure at high strain rates that can be obtained via laser shocks; in this regime pre-existing defects in the material play a minor role in spall failure.[5] The similarity of critical exponents for different metals and force fields suggests the universality of this phenomenon of failure under tension at high strain rates, which may also apply to cavitation.[18]

This research was funded by Grant No. DOE W-7405-ENG-48 from DOE-ASCI-ASAP. The facilities of the MSC are also supported by grants from NSF (MRI CHE 99), ARO (MURI), ARO (DURIP), NASA, BP Amoco, Exxon, Dow Chemical, Seiko Epson, Avery Dennison, Chevron Corp., Asahi Chemical, 3M, and Beckman Institute.

*Author to whom correspondence should be addressed.

[1] A. K. Zurek, W. R. Thissell, J. N. Johnson, D. L. Tonks, and R. Hixson, J. Mater. Process. Technol. **60**, 261 (1996).

[2] T. de Rességuier, S. Couturier, J. David, and G. Niérat, J. Appl. Phys. **82**, 2617 (1997).

[3] L. Tollier, R. Fabbro, and E. Bartnicki, J. Appl. Phys. **83**, 1224 (1998); L. Tollier and R. Fabbro, *ibid.* **83**, 1231 (1998).

[4] E. Moshe *et al.*, J. Appl. Phys. **83**, 4004 (1998).

[5] E. Dekel *et al.*, J. Appl. Phys. **84**, 4851 (1998).

[6] E. Moshe *et al.*, Appl. Phys. Lett. **76**, 1555 (2000).

[7] N. J. Wagner, B. L. Holian, and A. F. Voter, Phys. Rev. A **45**, 8457 (1992); J. Belak, J. Comput.-Aided Mater. Des. **5**, 193 (1998).

[8] D. L. Tonks, J. Phys. IV **4**, 665 (1994).

[9] M. Ortiz and A. Molinari, J. Appl. Mech. **59**, 48 (1992); P. F. Thomason, Acta Mater. **47**, 3633 (1999).

[10] Alejandro Strachan, Tahir Çağın, Oğuz Gülseren, Sonali Mukherjee, R. E. Cohen, and William A. Goddard III (unpublished). This FF was fitted to the QM calculations for bcc, fcc, and A15 phases of Ta over a range of pressure from $\sim$ 500 GPa (compression) to ~ -10 GPa.

[11] H. Ikeda, Y. Qi, T. Çağın, K. Samwer, W. L. Johnson, and W. A. Goddard III, Phys. Rev. Lett. **82**, 2900 (1999); T. Çağın, Y. Qi, H. Li, Y. Kimura, H. Ikeda, W. L. Johnson, and W. A. Goddard III, in *Bulk Metallic Glasses*, edited by A. Inoue, W. L. Johnson, and C. T. Liu (Materials Research Society, Warrandale, 1999), p. 43.

[12] F. Milstein, J. Appl. Phys. **44**, 3825 (1973).

[13] Dietrich Stauffer, *Introduction to Percolation Theory* (Taylor & Francis, London and Philadelphia, 1985).

[14] M. E. Fisher, Physics (N.Y.) **3**, 255 (1967); Rep. Prog. Phys. **30**, 615 (1967).

[15] P. F. Mastinu *et al.*, Phys. Rev. Lett. **76**, 2646 (1996).

[16] C. O. Dorso, V. C. Latora, and A. Bonasera, Phys. Rev. C **60**, 034606 (1999).

[17] J. A. Astrom, B. L. Holian, and J. Timonen, Phys. Rev. Lett. **84**, 3061 (2000).

[18] W. B. McNamara, Y. T. Didenko, K. S. Suslick, Nature (London) **401**, 772 (1999).